225. Fragmentation of Energy Selected Butadiyne- and 1,3-Pentadiyne Radical Cations

by **Josef Dannacher, Edgar Heilbronner, Jean-Pierre Stadelmann** and **Jürgen Vogt**

Physikalisch-chemisches Institut der Universität Basel, Klingelbergstrasse 80, CH-4056 Basel

Dedicated to Professor Edgardo Giovannini on the occasion of his seventieth birthday

(17.VIII.79)

Summary

Monomolecular fragmentations of butadiyne- and 1,3-pentadiyne radical cations in their electronically excited states have been investigated by use of the photoelectron-photoion coincidence technique. Breakdown curves for the molecular and various fragment ions have been recorded over the ionization energy range of 9 to 17 eV. These breakdown curves reveal the extent of the competition between the radiative relaxation (ion fluorescence) and the non-radiative internal conversion followed by fragmentation for the decay of the first excited electronic states. Extensive hydrogen scrambling and/or ionic-carbon-skeleton isomerization takes place prior to fragmentation, as revealed by the breakdown curves obtained for the site specifically deuteriated 1,3-pentadiynes.

Introduction. – For a long time, the emission spectrum of butadiyne radical cation, corresponding to the transition $\tilde{A}^2\Pi_u \rightarrow \tilde{X}^2\Pi_g$ has been the only one known for a polyatomic radical cation consisting of more than three atoms [1]. However, in the course of recent investigations by *Maier et al.* [2] of the radiative decay of organic molecular radical cations in the gas phase, the emission spectra of several alkyl substituted diacetylene radical cations have been recorded, *e.g.* 1,3-pentadiyne and its deuterioderivatives, 1,3-hexadiyne, 2,4-hexadiyne and its deuterioderivatives, and finally 3,5-octadiyne.

Quite generally it was found that only for few radical cations the radiative and dissociative relaxation channels are in effective competition [3] [4]. This follows from a comparison of results derived from the emission spectra with the information concerning the lowest fragment ion appearance energy *(AE)* obtained from photoionization (PI) or electron impact (EI) measurements.

Photoelectron-photoion coincidence spectroscopy is one of the techniques of choice for the study of the fate of excited molecular ions prepared in states with various, but precisely known internal energies E^* (= total energy, relative to the electronic and vibrational ground state of the ion). The ratios $[M^+]_t/[M^+]_0$ and $[F^+(m_k)]_t/[M^+]_0$, *i.e.* the amount of parent ion $[M^+]_t$ or the amounts of fragment

0018-019X/79/7/2186-16$01.00/0

ions $[F^+(m_k)]_t$ after time t, relative to the amount $[M^+]_0$ of undissociated parent ion M^+ at time zero are unambiguously obtained as a function of E^*, *i.e.* as a function of those ionization energies I which are accessible in the range provided by the photon source used (*e.g.* the range 0 to ~20 eV with a He($I\alpha$) source). For example, 2,4-hexadiyne radical cation has recently been investigated by this technique [4] and has been shown to be one of the few examples exhibiting competition between radiative and dissociative decay.

Problem. – This paper is concerned with the radical cations of the following molecules, in particular **2** and its deuterium labeled derivatives **2**(D,H), **2**(H,D) and **2**(D,D):

x–C≡C–C≡C–x	**1**(x)	x = H or D
x–C≡C–C≡C–Cy_3	**2**(x,y)	x,y = H and/or D
H_3C–C≡C–C≡C–CH_3	**3**	

A superscript «+» denotes the corresponding radical cation and, if necessary, its electronic state is quoted in parentheses, *e.g.* $\mathbf{2}^+(H,D;\tilde{A})$ refers to H–C≡C–C≡C–CD_3^+ in its $\tilde{A}(^2E)$ state.

In this work we attempt to contribute towards a solution of the following two problems:

a) It is known that the decay behaviour of $\mathbf{1}^+$ in its first excited electronic state $\tilde{A}(^2\Pi_u)$ is characterized by the fact that only the radiative (rad.) and the nonfragmenting non-radiative (nrad.) channels are available:

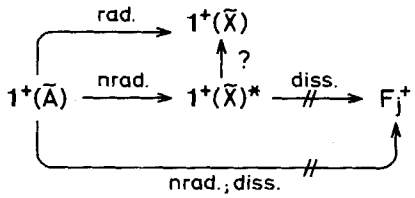

(1)

In the diagram (1), the symbol $\mathbf{1}^+(\tilde{X})^*$ stands for the vibrationally highly excited radical cation $\mathbf{1}^+$ in its electronic ground state $\tilde{X}(^2\Pi_g)$ and F_j^+ for fragment ions. It should be realized that (1) is only a crude, first approximation to the very involved decay mechanism. On the other hand it was known that radiative, nonradiative and dissociative channels are available to $\mathbf{3}^+$ in its first electronically excited state [4].

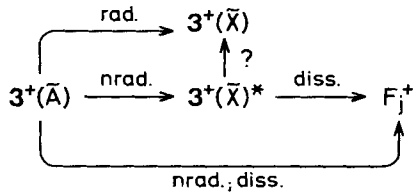

(2)

On the basis of the literature value for the lowest fragment ion AE of **1** available when this investigation was started (12.1±0.3 eV [5]) and of the emission spectrum

of $\mathbf{1}^+$ [1] [6] one might have predicted the same behaviour for $\mathbf{1}^+(\tilde{A})$ as the one shown for $\mathbf{3}^+(\tilde{A})$ in (2). In the course of the present study it turned out that this AE was considerably in error. Note that both states $\tilde{A}$ correspond to electronic excitation within the π-manifold of states, *i.e.* for $\mathbf{1}^+$: $\tilde{A} = {}^2\Pi_u$, for $\mathbf{3}^+$: $\tilde{A} = {}^2E_u$.

By analogy to **3**, the presence of a methyl group in $\mathbf{2}^+(H,H)$ would lead to the conclusion that this radical cation in its $\tilde{A}$-state should also behave according to (2) rather than to (1). As we shall see, this is indeed the case.

b) Solving problem a) leads necessarily to the question whether the two types of H-atoms in $\mathbf{2}^+(H,H)$ behave differently, *i.e.* whether the dissociation process

$$\mathbf{2}\,(H,H;\tilde{A}) \longrightarrow\longrightarrow\longrightarrow H\text{-}C{\equiv}C\text{-}C{\equiv}C\text{-}CH_2^+ + H \qquad (3)$$
$$\downarrow ?$$

is preferred over the dissociation process

$$\mathbf{2}\,(H,H;\tilde{A}) \longrightarrow\longrightarrow\longrightarrow C{\equiv}C\text{-}C{\equiv}C\text{-}CH_3^+ + H, \qquad (4)$$

always assuming that such a structural representation of the H-atom loss starting from an electronically excited state of the parent ion is at least an acceptable approximation for the rate determining step. To investigate this problem the labeled compounds **2**(H, D), **2**(D, H) and **2**(D, D) have been included.

Results and Discussion. – Consider the parent ion M^+ of internal energy E^* corresponding to a particular ionization energy I. The ratio of the amount of fragment ions of mass m_k detected after a sampling time t, $[F^+(m_k)]_t$, relative to the amount of parent ions formed at time zero, $[M^+]_0$ constitutes the branching ratio

$$b[I, m_k]_t = [F^+(m_k)]_t / [M^+]_0. \qquad (5)$$

A plot of $b[I, m_k]_t$ as a function of I is referred to as the breakdown curves for the corresponding parent and fragment ions. From definition (5) follows that

$$\sum_{M^+ \text{ and } F^+(m_k)} b[I, m_k]_t = 1 \qquad (6)$$

so that the sum of all breakdown curves should yield a horizontal line with ordinate unity for all values of the abscissa I. Consequently, deviations of the experimental sum curve from expectation (6) indicate nonideal behaviour of the spectrometer, owing to its discrimination against high kinetic energy fragments (which are not all recorded) and/or low fragment formation rates, *i.e.* rates which would give rise to metastable ions in traditional mass spectrometry.

Butadiyne **1***(H).* The He(Iα) photoionization mass spectrum of **1**(H) consists of the signals of the parent ion $M^+ = C_4H_2^+$ ($m/z = 50$; rel. int. 100%) and of the only accessible fragment ion C_4H^+ ($m/z = 49$; rel. int. 55%), formed by loss of a H-atom. The photoelectron spectrum of **1**(H) recorded under low-resolution coincidence conditions exhibits three bands within the accessible ionization energy region *(cf. Fig. 1)* which have been assigned by *Baker & Turner* [7] as follows: ① $\tilde{X}\,{}^2\Pi_g$; ② $\tilde{A}\,{}^2\Pi_u$; ③ $\tilde{B}\,{}^2\Sigma_g$. The coincidence spectrum shown in the same figure indicates that $\mathbf{1}^+(H;\tilde{X})$ and $\mathbf{1}^+(H;\tilde{A})$ do not fragment, the corresponding branching ratios

$b[I, M^+]_t$ for the parent ion being unity within the limits of error of the counting statistics. This result is confirmed by the lack of observable coincidences between electrons corresponding to band ② and C_4H^+ fragments, notwithstanding the fact that such coincidences have been looked for with significantly improved counting statistics. This result excludes that $b[I, C_4H^+] > 0.003$ for ~ 12 eV $< I < \sim 13$ eV, *i.e.* the ionization energy range of the $\tilde{A}\,^2\Pi_u$ state of $\mathbf{1}^+(H)$. Obviously, this result disagrees with the previously reported appearance energy $AE = 12.1 \pm 0.3$ eV for the loss of a H-atom [5]. Indeed, a remeasurement of the appearance energy of the fragment C_4H^+ resulted in AE = 15.9 ± 0.2 eV [8], a value in agreement with the coincidence spectrum shown in *Figure 1*. Furthermore, the latter value is also in excellent agreement with a calculated value $AE \approx 16.0$ eV obtained under the assumption that the dissociation energy for the process $\mathbf{1}^+(H; \tilde{X}) \rightarrow C_4H^+ + H$ has the same value $D_0 = 5.8$ eV as the loss of a H-atom by the acetylene radical cation in its electronic ground state, *i.e.* $C_2H_2^+(\tilde{X}) \rightarrow C_2H^+ + H$. The latter value is the difference between the appearance energy $AE(C_2H^+/C_2H_2) = 17.2$ eV [9] [10] and the ionization energy of acetylene $I_1 = 11.4$ eV [9]. Note that the value $D_0 = 5.8$ eV for $\mathbf{1}^+(H; \tilde{X}) \rightarrow C_4H^+ + H$ is presumably an upper limit, because the positive charge in $\mathbf{1}^+(H; \tilde{X})$ and C_4H^+ is distributed over two acetylene moieties and because the dissociation energy for the process $C_2H_2 \rightarrow C_2H + H$ involving the neutral acetylene molecule is only $D_0 = 5.2$ eV [9]. It follows from the above analysis that the dissociative pathway is inaccessible for $\mathbf{1}^+(H; \tilde{A})$.

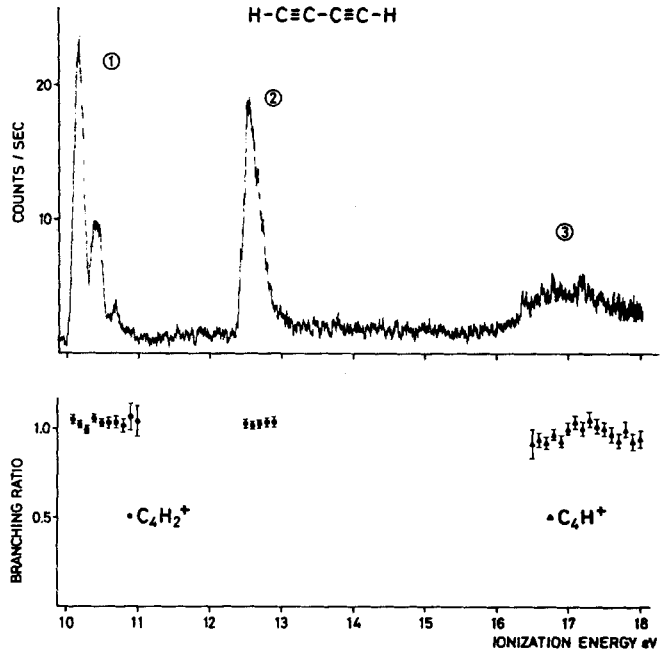

Fig. 1. *He(Ia) PE-spectrum of butadiyne* **1***(H) under coincidence conditions and the breakdown curves for the* $C_4H_2^+$ *parent ion (●) and the* C_4H^+ *fragment ion (▲).* The bars in this and the succeeding figures correspond to the standard deviation of the counting statistics.

The analysis of the vibrational fine structure of the second band in the photoelectron spectrum of **1**(H), which corresponds to the $\tilde{A}^2\Pi_u$ state of the radical cation $\mathbf{1}^+$(H), shows that at least eight vibrationally excited states of the latter are populated upon He(Iα) photoionization, apart from the vibrational ground state. The vibrational modes involved are ν_1, ν_2, ν_3, using the nomenclature proposed by *Herzberg* [11]:

	$\mathbf{1}^+(\tilde{X})$ [11]	$\mathbf{1}^+(\tilde{A})$ [7] [11]	
ν_1: C–H stretch; sym. $\tilde{\nu}_1/cm^{-1}$	3137	2858	
ν_2: C≡C stretch; sym. $\tilde{\nu}_2/cm^{-1}$	2177	1860	(7)
ν_3: C–C stretch; sym. $\tilde{\nu}_3/cm^{-1}$	861	810	

In order of increasing energy the populated states of $\mathbf{1}^+(\tilde{A})$ are: (0,0,0), (0,0,1), (0,0,2), (0,1,0), (0,0,3), (0,1,1), (1,0,0), (0,0,4) and (0,1,2). Usually, rapid internal conversion is the preferred pathway for the depletion of electronically excited states. However, in the case of $\mathbf{1}^+$(H; $\tilde{A}$), the emission spectra [1] [6] [12] reveal that radiative decay competes with internal conversion in depleting the vibrational states (0,0,0), (0,0,1), (0,0,2) and (1,0,0) of $\mathbf{1}^+$(H; $\tilde{A}$). It is probable that the remaining vibrational states also decay radiatively, but that the corresponding emission bands remain undetected because of overlap with other, stronger emission bands and/or because of their low intensity. An increase of the rate of internal conversion with increasing vibrational excitation is suggested by the corresponding lifetimes *(cf. Table 1)* if one assumes that the radiative rate is constant [6]. This increase is readily explained by the higher vibrational state density of the particular electronic state (*i.e.* usually $\tilde{X}$) to which the internal conversion occurs.

Replacing the H-atoms in **1**(H) by deuterium, to yield **1**(D), should result in two effects, namely a general increase in the densities of vibrational states and a

Table 1. *Radiative rates* (k_r) *and non-radiative rates* (k_{nr}), *as deduced* (see text) *from the branching ratios for the parent ions of the butadiynes* **1***(H) and* **1***(D) measured at* $1 = 12.4$ *eV, and of the 1,3-pentadiynes* **2***(H,H),* **2***(D,H),* **2***(H,D) and* **2***(D,D) measured at* $1 = 12$ *eV.* The life-times τ are taken from the emission study described in [2].

Compound	State	τ/ns	Branching ratio of M^+	$(k_r/s^{-1}) \cdot 10^7$	$(k_{nr}/s^{-1}) \cdot 10^7$
1(H) H–C≡C–C≡C–H	$\tilde{A}^2\Pi_u$ 0^0	71 ± 3	1.0	1.41	
	3^1	61 ± 3			
1(D) D–C≡C–C≡C–D	$\tilde{A}^2\Pi_u$ 0^0	78 ± 4	1.0	1.28	
	3^1	69 ± 4			
2(H,H) H–C≡C–C≡C–CH_3	$\tilde{A}^2E$ 0^0	48 ± 3	0.76 ± 0.06	1.6	0.5
	$7^1, 6^1$	46 ± 3			
2(D,H) D–C≡C–C≡C–CH_3	$\tilde{A}^2E$ 0^0	46 ± 3	0.73 ± 0.01	1.6	0.6
	$7^1, 6^1$	45 ± 3			
2(H,D) H–C≡C–C≡C–CD_3	$\tilde{A}^2E$ 0^0	51 ± 3	0.79 ± 0.06	1.5	0.4
	7^1	51 ± 3			
2(D,D) D–C≡C–C≡C–CD_3	$\tilde{A}^2E$ 0^0	53 ± 3	0.82 ± 0.01	1.5	0.3
	7^1	53 ± 3			

change in the *Franck-Condon* factors. As shown in *Table 1* the life-times of $\mathbf{1}^+$(D; $\tilde{A}$) are larger than those of $\mathbf{1}^+$(H; $\tilde{A}$). This suggests that the changes in the *Franck-Condon* factors overcompensate the effect due to an increased vibrational state density, which by itself would result in a shortening of the life-times.

It should be mentioned, that internal conversion from $\mathbf{1}^+$(H; $\tilde{A}$) to $\mathbf{1}^+$(H; $\tilde{X}$) could also occur *via* other, non-*Koopmans* states of the radical cation. Indeed, INDO-CI calculations perfomed by *Čársky, Kuhn & Zahradník* [13] yield three such electronic states ($^4\Pi_u$, $^2\Pi_u$, $^2\Phi_u$) within the energy interval between the $\tilde{X}\,^2\Pi_g$ and $\tilde{A}\,^2\Pi_u$ (dominantly *Koopmans*) states of $\mathbf{1}^+$(H). However, in the absence of more detailed information, their role in the decay mechanism of $\mathbf{1}^+$(H; $\tilde{A}$) remains unknown.

Looked at from the point of view of our coincidence experiments it is unfortunate that the $\tilde{A}\,^2\Pi_u$ states of **1**(H) and **1**(D) lie at lower energies than the lowest fragmentation threshold. Therefore nothing can be deduced from the (trivial) breakdown curves, concerning the competition between radiative and non-radiative decay mechanisms. On the other hand the coincidence spectrum for the C_4H^+ fragment (see *Fig. 1*) shows, that the parent ions $\mathbf{1}^+$(H) formed with an internal energy corresponding to the range of ionization energies of the photoelectron band ③, *i.e.* of $\mathbf{1}^+$(H; $\tilde{B}$) dissociate according to $\mathbf{1}^+(H) \rightarrow C_4H^+ + H$ within the time-scale of our experiment.

1,3-Pentadiynes **2**(*x,y*), *x,y=H and/or D.* The photoelectron spectrum of **2**(H,H) recorded under coincidence conditions is shown in *Figure 2.* The low electron count rate is a consequence of having chosen conditions for an optimum ionization rate, demanded by the coincidence experiment. The constant electric field applied in the ionization source, together with the slitwidth used in the electron analyzer are at the origin of the poor resolving power. On the basis of a high-resolution photoelectron spectrum of **2**(H,H) [14], the two bands ① and ② and the band system ③ have been assigned as follows (under C_{3v} symmetry):

Band	①	②	③		
State	$\tilde{X}\,^2E$	$\tilde{A}\,^2E$	$\tilde{B}\,^2A_1$	$\tilde{C}\,^2E$	$\tilde{D}\,^2A_1$
I/eV	9.51	12.02	14.6	15.5	16.8

(8)

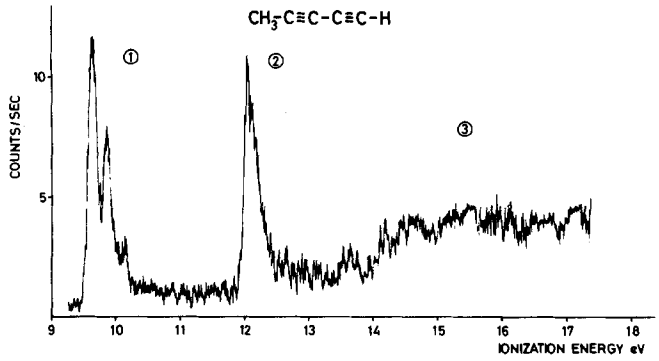

Fig. 2. *He(Iα) photoelectron spectrum of 1,3-pentadiyne* **2**(*H,H*) *recorded under coincidence conditions*

The ionization energies I quoted for ① and ② are the adiabatic values, whereas the vertical ionization energies (approximated by the positions of the band maxima) are quoted for the three components of ③. The same energies, as given in (8), are valid for the isotopically labeled compounds **2**(D,H), **2**(H,D) and **2**(D,D).

Mass spectral data for **2**(x,y), x,y = H and/or D, obtained by He(Iα)-photoionization or electron impact are collected in *Table 2*. The following scheme summarises the observed fragmentations:

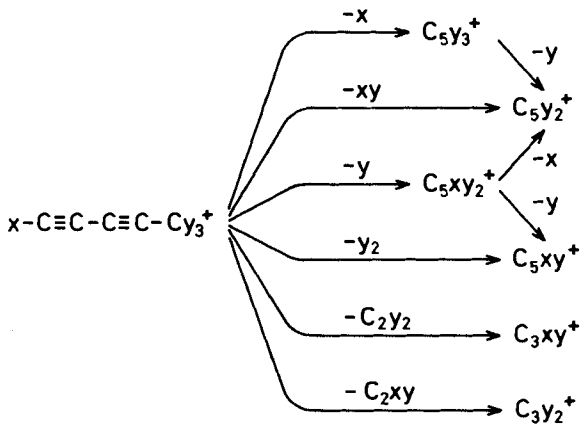

Table 2. *Mass spectral data for the 1,3-pentadiynes* **2**(*H,H*), **2**(*H,D*), **2**(*D,H*) *and* **2**(*D,D*). F_s denotes the source field strength and f_i the ion collection efficiency for thermal parent ions. EI = electron impact, PI = photoionization, using He(Iα) radiation.

Ion	EI[a])	EI[b])	PI			
	2(H,H)	**2**(H,H)	**2**(H,H)	**2**(D,H)	**2**(H,D)	**2**(D,D)
M^+	100	100	100	100	100	100
$M^+ - H$	55	45	60	55	23	–
$M^+ - D$	–	–	–	18[c])	41	55
$M^+ - H_2$	20	9	25	12[c])	–	–
$M^+ - HD$	–	–	–	10	10	–
$M^+ - D_2$	–	–	–	–	8	20
$M^+ - C_2H_2$	10	7	8	9	–	–
$M^+ - C_2HD$	–	–	–	7	3	–
$M^+ - C_2D_2$	–	–	–	–	5	21
Summed intensities for the loss of						
– one atom			60	73	63	55
– two atoms			25	22	18	20
– an acetylene molecule			8	16	8	21
Total fragment ion intensity			93	111	90	96
F_s(V cm^{-1})			4.85	5.54	4.85	5.54
f_i			0.25	0.38	0.28	0.34

[a]) Instrument: *Hitachi Perkin-Elmer* RMU-7D, 70 eV, 10 μA emission current.
[b]) Same as a) but ~20 eV.
[c]) Concerning the partition of the $m/z = 63$ intensity, see text.

There are three categories of fragmentations involving (i) the loss of a single atom (x or y); (ii) loss of an acetylene molecule (C_2xy or C_2y_2), and (iii) loss of a diatomic (xy or y_2).

At high internal energies this last reaction proceeds also *via* a consecutive loss of two atoms. At the bottom of *Table 2* the summed intensities are given for each reaction category. In the case of **2**(D,H) the summed intensity for loss of a single H or D atom, *i.e.* $\mathbf{2}^+(D,H)-H$ and $\mathbf{2}^+(D,H)-D$ is about 20% higher than in the three other species. The increase of the intensity of the acetylene loss in $\mathbf{2}^+(D,H)$ and $\mathbf{2}^+(D,D)$ compared to $\mathbf{2}^+(H,H)$ and $\mathbf{2}^+(H,D)$ may be an artefact which could be attributed to the use of a higher source field for **2**(D,H) and **2**(D,D) *(cf. Table 2)* reducing the loss of high kinetic energy fragment ions. Since the mass ratio of the charged and the neutral fragment determines the partitition of the kinetic energy released, only loss of an acetylene can lead to high kinetic energy fragment ions.

In the case of **2**(D,H), M^+-D and M^+-2H both lead to fragment ions with $m/z=63$, but the relative contribution of the two processes can be inferred from the coincidence data of **2**(H,H), **2**(H,D) and **2**(D,D), discussed below.

For convenience the coincidence spectra *(Fig. 3–6)* are discussed in the next sections for each state separately.

$\mathbf{2}^+$, *Electronic ground state* $\tilde{X}\,^2E$ *(band ①)*: $\mathbf{2}^+(x,y;\tilde{X})$ cannot dissociate for energetic reasons as evidenced by the branching ratio $b[I,M^+]\approx 1$ for the parent ion ($I\approx 9.6$ to 10.3 eV).

Decay of $\mathbf{2}^+$ *(x, y; Ã) (band ②).* Coincidences with parent ions are detected in the entire energy range of the PE-band ②, *i.e.* corresponding to the $\tilde{A}\,^2E$ state. The parent ion breakdown curve decreases with increasing ionization energy *(cf. Fig. 3–6).* The relevant emission data are summarized in *Table 1.* Fluorescence has been detected from the zeroth vibrational level and for the 7^1 (symmetric C–C stretch) level of the $\tilde{A}\,^2E$ state of all four species. In the case of **2** (H,H) and **2** (D,H) emission from the 6^1 (asymm. C–C stretch) level was also observed [2]. Thus, only the lowest vibrational levels of the $\tilde{A}\,^2E$ state are known with certainty to decay radiatively. Therefore the parent ion branching ratio at the onset of band ②, (12.0 eV) was taken as the upper limit for the quantum yield of emission. The lack of detectable emission from higher excited levels might be due, as in the case of $\mathbf{1}^+(H)$, to very low intensities and/or overlapping with other lines of the band system. Internal conversion to a non or very slowly fragmenting state with respect to the time scale of our experiment as an alternative decay mechanism of $\mathbf{2}^+(x,y;\tilde{A})$ seems unlikely but cannot be completely ruled out since the coincidence experiment does not identify the electronic and/or the geometric structure of the detected molecular ions. Indeed, the near unity value of the sum curves and the symmetric time-of-flight distributions of the fragment ions argue for the absence of metastable molecular ions. The very weak metastable signal for the $\mathbf{2}^+(H,H)-H$ process, detected in the defocussed [15] EI mass spectrum, stems most probably from molecular ions formed *via* autoionization near the threshold energy.

The *AE* of $C_5H_3^+$ from **2**(H,H) was determined by electron impact as 11.6 ± 0.2 eV, *i.e.* about half an eV below the adiabatic ionization energy of the

$\tilde{A}\,^2E$ state. Thus, parent ions initially formed in the $\tilde{A}\,^2E$ state, which were not stabilized by fluorescence may dissociate after internal conversion of the electronic excitation energy. Taking the difference between $AE(C_5H_3^+/\mathbf{2}(H,H)) = 11.6$ eV and the adiabatic ionization energy of **2**(H,H), $I_a = 9.5$ eV, as C–H dissociation energy of $\mathbf{2}^+(H,H)$ to yield $H + HC{\equiv}C{-}C{\equiv}C{-}CH_2^+$, the value of $D_0(C{-}H) \approx 2.1$ eV is in exact agreement with the corresponding value for propyne (using *Lossing*'s value for $\Delta_f H^\ominus(HC{\equiv}C{-}CH_2^+) = 1176$ kJ mol^{-1} [16], $\Delta_f H^\ominus(HC{\equiv}C{-}CH_3) = 185$ kJ mol^{-1} [9] and $I_a(HC{\equiv}C{-}CH_3) = 10.36$ eV [17]). We interpret this rather striking similarity as evidence that the $C_5H_3^+$-fragment ion retains its open chain structure and does not isomerize at the threshold energy. In contrast, the $C_3H_3^+$ fragment ion from

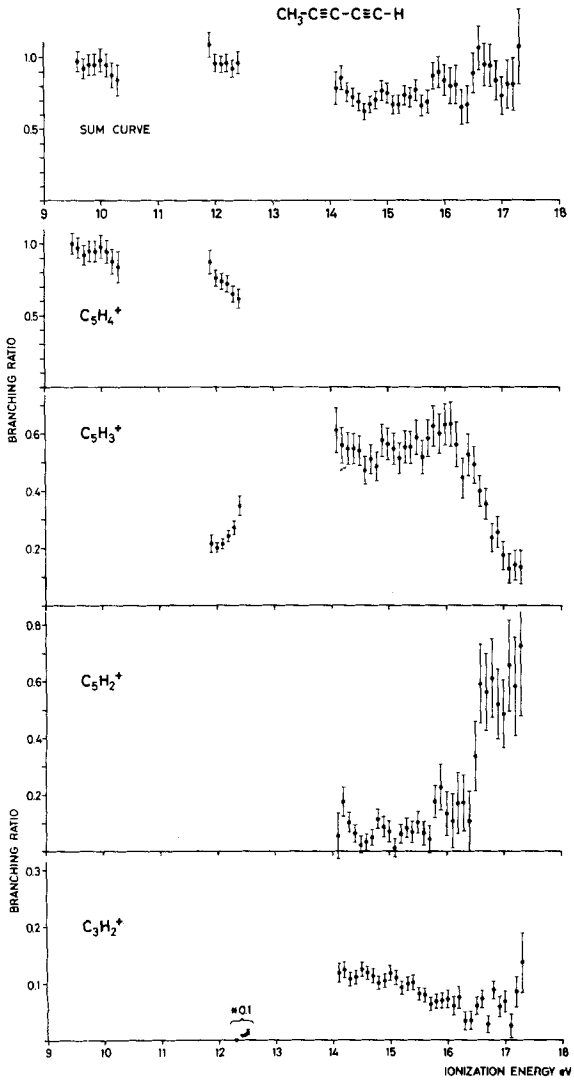

Fig. 3
Breakdown curves for the fragmentation of 1,3-pentadiyne radical cation $\mathbf{2}^+(H,H)$

propyne is formed as cyclopropenyl cation already at threshold [16] [18]. $\Delta_f H^{\ominus}(C_5H_3^+)$ can be calculated from $AE(C_5H_3^+/\mathbf{2}(H,H)) = 11.6$ eV and the estimated $\Delta_f H^{\ominus}(\mathbf{2}(H,H)) = 416$ kJ mol^{-1} [19]. The obtained value $\Delta_f H^{\ominus}(C_5H_3^+) = 1317$ kJ mol^{-1} is considerably lower than the upper limit of $\Delta_f H^{\ominus}(C_5H_3^+/\mathbf{3}) = 1431$ kJ mol^{-1} as reported by *Baer et al.* [20]. This difference might result from different fragment ion structures of $C_5H_3^+$, generated from **2**(H,H) as H–C≡C–C≡C–CH_2^+ and from **3** as H_3C–C≡C–C≡C^+. The breakdown curves for the loss of x and y from

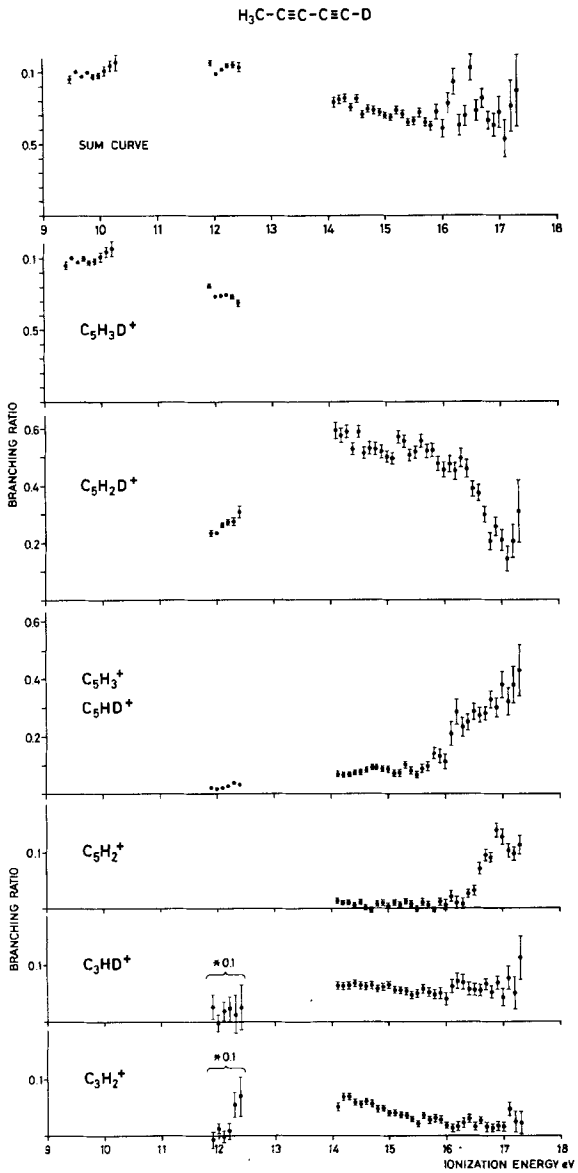

Fig. 4
Breakdown curves for the fragmentation of (1-d_1)-1,3-pentadiyne radical cation $\mathbf{2}^+(D,H)$

$2^+(D,H)$ and $2^+(H,D)$ clearly indicate that both these fragmentation channels are accessible for molecular ions formed in the $\tilde{A}\,^2E$ state. The most simple model assuming only loss of y (H or D) from the methyl group must therefore be discarded. On the other hand, a purely statistical treatment including an isotopic factor hardly explains the very different slopes of the M^+-x and the M^+-y breakdown curves, indicating a positional dependence.

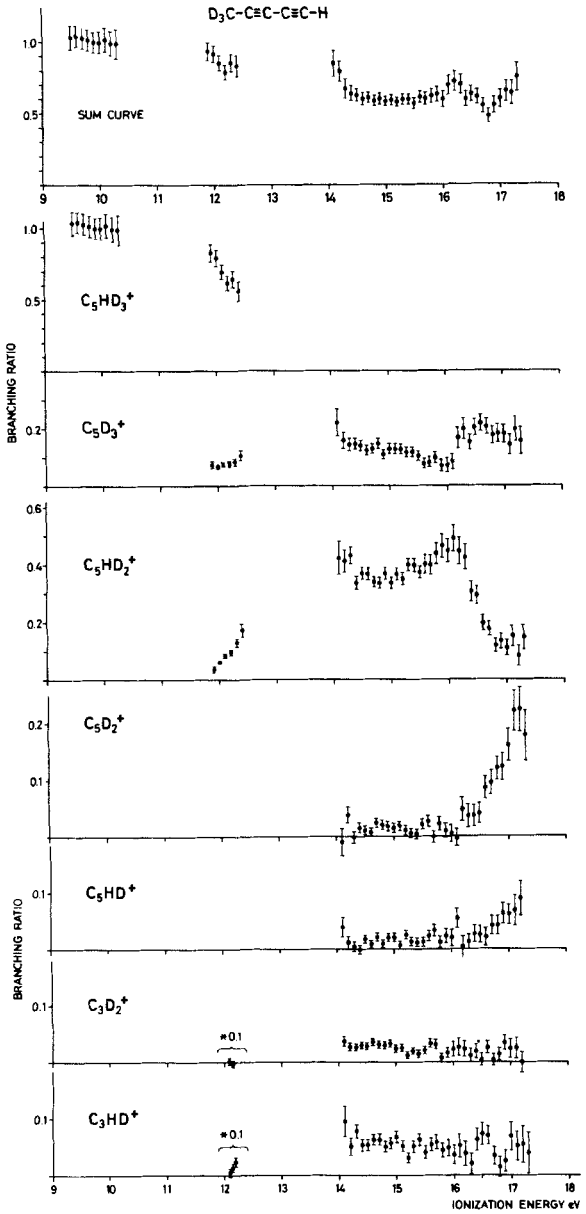

Fig. 5
The breakdown curves for the fragmentation of (5,5,5-d_3)-1,3-pentadiyne radical cation $2^+(H,D)$

The coincidence data can be reasonably interpreted using the model of *Howe & McLafferty* [21]. In this model it is assumed that the loss of x can only occur after a preceding scrambling process. The degree of scrambling is represented by α.

The results are collected in *Table 3.* The experimental ratios for H *vs.* D loss from $2^+(D,H;\tilde{A})$ and $2^+(H,D;\tilde{A})$ are obtained from the corresponding breakdown curves (*Fig. 4* and *5*). The values at 11.9 eV and at 12.4 eV are not considered since owing to the very low photoelectron signal these have significantly larger standard deviations than the four other values. The fairly constant value of $\alpha = 0.8$

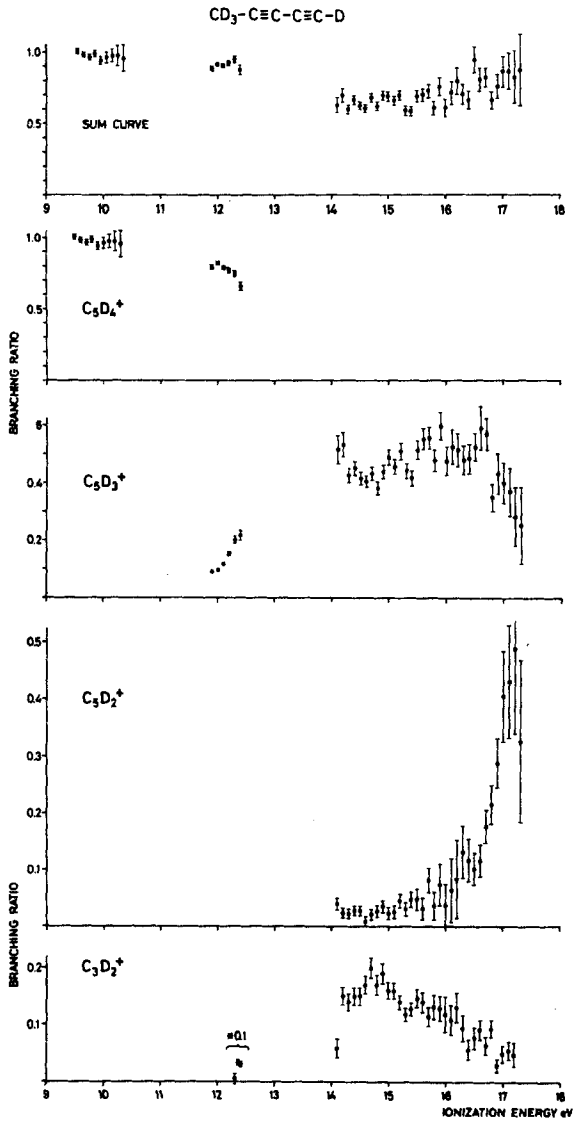

Fig. 6
The breakdown curves for the fragmentation of perdeuterio-1,3-pentadiyne radical cation $2^+(D,D)$

Table 3. *Rationalisation of the experimental* $M^+ - H$ vs. $M^+ - D$ *intensity ratio computed for* **2***(D,H) and* **2***(H,D) through a model with a scrambling factor* a *and an isotope effect factor* k_H/k_D, *taken at four selected internal energies* E^* *of the* $\tilde{A}\,(^2E)$ *state.* For further details see text and [26]

Ionization energy I in eV	Intensity $(M^+ - H)$/ Intensity $(M^+ - D)$		Degree of scrambling a	Isotope effect k_H/k_D
	$2^+(D,H)$	$2^+(H,D)$		
12.0	10.5	0.71	0.84	2.9
12.1	11.4	0.64	0.79	2.9
12.2	8.9	0.62	0.85	2.5
12.3	7.2	0.46	0.81	1.9

reflects the high degree of scrambling at these low internal energies of the molecular ion. The isotope effect decreases from ~3 to ~2 with increasing internal energy. Similar values for a and i were found in other cases [21]. Besides the loss of a single H- or D-atom there is another fragmentation channel which is loss of acetylene accessible within the $\tilde{A}\,^2E$ state. The AE of this process was found to be 12.3 ± 0.2 eV, equal within the limits of error for all the four labeled species **2**. Two isotopic acetylene molecules can be formed from **2**(D,H) and **2**(H,D), *i.e.* C_2xy and C_2y_2. However, only the process leading to the neutral acetylene molecule containing the maximum number of D-atoms (*i.e.* C_2HD from $2^+(D,H;\tilde{A})$ and C_2D_2 from $2^+(H,D;\tilde{A})$) is observed. The structure of the corresponding fragment ions C_3xy^+ or $C_3y_2^+$ remains unknown, but its formation necessitates at least one H- or D-shift.

The EI determination of $AE(C_3H_2^+/\mathbf{2}(H,H))$ yielded 13.1 eV, *i.e.* 0.8 eV higher than the corresponding coincidence value. We interpret this difference as due to the rather low abundance of that fragment ion, which tends to increase the EI-AE value, and the much higher intrinsic sensitivity of the coincidence method compared to conventional EI and PI techniques. Similar significant differences between photoelectron-photoion coincidence and PI-appearance energy data have been reported by *Stockbauer et al.* [22] [23]. With $\Delta_f H^\ominus(\mathbf{2}) = 416$ kJ mol^{-1} [19] as used above and $\Delta_f H^\ominus(HC{\equiv}CH) = 227$ kJ mol^{-1} [9] one obtains from the reaction

$$C_5H_4^+ \xrightarrow[12.3\text{ eV}]{AE(C_3H_2^+)} C_3H_2^+ + C_2H_2$$

$\Delta_f H^\ominus = (C_3H_2^+) = 1376$ kJ mol^{-1}. This value is considerably lower than the corresponding values for $\Delta_f H^\ominus(C_3H_2^+)$ from allene (coincidence: 1450 kJ mol^{-1}, PI: 1494 kJ mol^{-1} [22]), or from propyne (coincidence: 1443 kJ mol^{-1}, PI: 1505 kJ mol^{-1} [23]). The presence of excess energy in this fragmentation would increase our value for $\Delta_f H^\ominus(C_3H_2^+)$, implying that either the estimated $\Delta_f H^\ominus(C_5H_4)$ is too high by about 65 kJ mol^{-1} or that the H_2-elimination from allene- and propyne-radical cations involves excess energies of the mentioned magnitude.

Higher excited electronic states (band ③). In this energy range no molecular ions have been detected in coincidence. Loss of y remains the dominant fragmentation pathway up to ~16 eV. Above this energy the breakdown curves corresponding to the loss of a single H- or D-atom decrease steeply, owing to the accessibility of the consecutive abstraction of two H/D-atoms. This is evidenced by the strong

increase of the breakdown curves of the various C_5xv^+ and $C_5y_2^+$ fragments. Except for **2**(D,H) a smooth increase in the M^+-y breakdown curves is detected around ~16 eV. The M^+-x process can be unambiguously observed only for **2**(H,D). The corresponding breakdown curve shows a step near ~16 eV. These features found in the M^+-x and M^+-y breakdown curves may well indicate a change of the processes leading to these ions, but the limited precision of the present coincidence data prevent a more detailed analysis.

The breakdown curve for $m/z=63$ of **2**(D,H) contains contributions from $C_5H_3^+$ and C_5HD^+. A qualitative deconvolution is possible using the data of the other three isotopic compounds **2**(x,y).

(i) Below 16.4 eV, C_5HD^+ can only be formed from **2**(D,H) by loss of an H_2-molecule. The branching ratio for this process can be estimated from the spectra of **2**(H,H), **2**(H,D) and **2**(D,D) to be ~0.02. Consequently the remaining intensity of ~0.06 below 16 eV can be ascribed to the formation of $C_5H_3^+$.

(ii) The step of b[*I*, $m/z=63$] at ~16.2 eV to about ~0.20 is assumed to reflect the same behaviour as found for M^+-x in the case of **2**(H,D).

(iii) The increase of b[*I*, $m/z=63$] above ~16.4 eV is due to the secondary process involving the consecutive abstraction of two H-atoms.

With these estimates the total relative intensity of $m/z=63$ of 30 percent observed in the mass spectrum of **2**(D,H) has been partitioned into 18% $C_5H_3^+$ and 12% C_5HD^+.

The abstraction of molecular hydrogen (H_2, HD or D_2) seems to be a very unfavourable decay channel, but as soon as there is enough energy for a consecutive abstraction of two atoms it becomes the most intense pathway. For ionization energies $I>16.5$ eV the loss of two H-atoms from **2**(D,H) is faster than the loss of H and D from **2**(D,H). The analogous kinetic isotope effect is observed for **2**(H,D) where loss of two D-atoms is the slower process.

The electron impact appearance energy of 13.7 eV for $C_5H_2^+/$**2**(H,H) fits well with the observed breakdown curve for the H_2-elimination. Moreover, a break in the EI-ionization efficiency curve was found at ~16.6 eV, corresponding to a similar break in the breakdown curve of this fragment ion at ~16.4 eV *(cf. Fig. 3)*, which originates from the stepwise elimination of two H-atoms. As already mentioned, the breakdown curves for the loss of acetylene are expected to be distorted by discrimination of high kinetic energy fragments. The low value of the sum curve within the energy range of band ③ is mainly attributed to this effect. The M^+-acetylene breakdown curves decrease with increasing ionization energy.

We wish to thank Dr. *Else Kloster-Jensen* for her advice concerning the synthesis and the purification of the acetylenic compounds used in this study, and Mrs. *Beatrice Bullen* for her help in preparing them. This work is part C4 of Project No. 2.518-0.78 of the *Schweizerischer Nationalfonds zur Förderung der wissenschaftlichen Forschung* (for Part C3 see [28]). Financial support by *Ciba-Geigy SA, Sandoz SA* and *F. Hoffmann-La Roche & Co. SA*, Basel, is gratefully acknowledged.

Experimental Part. – Photoelectron-Photoion Coincidence Spectrometer. The fixed wavelength photoelectron-photoion coincidence technique, which has been described in detail [24], can be summarised as follows: A collimated beam of He(Iα) radiation intersects a sample gas jet in the ioniza-

tion source. Photoelectrons and photoions are accelerated in opposite directions by a weak electrostatic field in the source region. The electrons are energy analyzed by a conventional 10 cm radius $\pi/\sqrt{2}$ cylindrical condenser analyzer with a typical resolving power $E/\Delta E = 50$ to 100, and a total electron collection efficiency $f_e \approx 10^{-4}$. The photoions pass through accelerating and focusing ion optics before entering a quadrupole mass spectrometer, which provides unity mass resolution over the accessible mass range, *i.e.* up to $m/z = 511$. The advantage of this experimental set-up compared to pure time-of-flight mass analysis is twofold. Firstly the investigation of organic radical cations necessitates that two ions are separable even when they differ by only one H-atom, *i.e.* one mass unit. Secondly, ions of other than the preselected mass are prevented to reach the detector and therefore cannot contribute to the random coincidence rate. This leads to improved counting statistics, a factor of some importance when dealing with less abundant ions which are otherwise hardly detectable. This is the reason why the inclusion of a quadrupole mass filter yields a superior experimental set-up, provided that a high transmission can be retained. This is realised in our spectrometer which has a typical ion collection efficiency for thermal ions of $f_i = 0.2$ to 0.5. To obtain the breakdown curves shown in *Figures 1–6*, the ionization energy was scanned with a scanning speed of order of magnitude 1 eV/day, the exact value depending on the desired signal to noise ratio. The raw data have been corrected for random coincidences, isotopic abundances, impurities and background pulses as described previously in [24].

Samples. – *Butadiyne* (**1**). Butadiyne was prepared by reacting 1,4-dichlorobutyne-2 with potassium hydroxide, as described in [25].

1,3-Pentadiyne (**2**(H,H)). 1,3-Pentadiyne was prepared from 1,4-dichlorobutyne-2 *via* elimination of hydrogen chloride using sodium amide, and subsequent methylation of the monosodium salt of butadiyne with methyliodide [25].

1-d_1-1,3-Pentadiyne (**2**(D,H)). 1-d_1-1,3-Pentadiyne was obtained from **2**(H,H) by isotopic exchange in a solution of NaOD in D_2O [26]. After two exchanges for about 90 min each, 70% of the acetylenic compound was recovered with an isotopic purity of better than 98%.

5,5,5-d_3-1,3-Pentadiyne (**2**(H,D)). 5,5,5-d_3-1,3-pentadiyne, containing about 4% of dideuteriated 1,3-pentadiyne, was prepared in analogy to **2**(H,H) by reacting the monosodium salt of **1** with trideuteriomethyl iodide.

1,5,5,5-d_4-1,3-Pentadiyne (**2**(D,D)). Perdeuterio-pentadiyne was obtained by isotopic exchange, starting from **2**(H,D) and using the procedure described for the preparation of **2**(D,H). The resulting sample was contaminated by about 3% of the starting material **2**(H,D).

Sample Preparation. All samples used in this investigation were purified by fractional bulb-to-bulb condensation and/or preparative gas-liquid-chromatography (Apiezon L, 15%, 50 to 90°) prior to use in the spectrometer.

Appearance Energies (AE). The electron impact appearance energies were determined by a modified second derivative method described previously [27] using a *Hitachi Perkin-Elmer* RMU-7D double focusing mass spectrometer.

REFERENCES

[1] *J. H. Callomon,* Canad. J. Physics *34*, 1046 (1956).
[2] *J. P. Maier, O. Marthaler & E. Kloster-Jensen,* Chem. Physics, in press.
[3] *M. Allan & J. P. Maier,* Chem. Physics Letters *43*, 94 (1976).
[4] *M. Allan, J. P. Maier, O. Marthaler & E. Kloster-Jensen,* Chem. Physics *29*, 331 (1978); *J. Dannacher,* Chem. Physics *29*, 339 (1978).
[5] *F. C. Coats & R. C. Anderson,* J. Amer. chem. Soc. *79*, 1340 (1957).
[6] *M. Allan, E. Kloster-Jensen & J. P. Maier,* Chem. Physics *17*, 11 (1976).
[7] *C. Baker & D. W. Turner,* Proc. Roy. Soc. *A 308*, 19 (1968).
[8] *U. Büchler,* Ph. D. Thesis, University of Basel 1978.
[9] *H. M. Rosenstock, K. Draxl, B. W. Steiner & J. T. Herron,* J. phys. chem. Reference Data *6*, Suppl. 1 (1977).

[10] *R. Botter, K.H. Dibeler, J.A. Walker & H.M. Rosenstock,* J. chem. Physics *44*, 1271 (1966).
[11] *G. Herzberg,* 'Electronic Spectra of Polyatomic Molecules', Van Nostrand Reinhold Company, New York, 1966.
[12] *W.L. Smith,* Proc. Roy. Soc. *A 300*, 519 (1967).
[13] *P. Čársky, J. Kuhn & R. Zahradník,* J. mol. Spectrosc. *55*, 120 (1975).
[14] *G. Bieri, F. Burger, E. Heilbronner & J.P. Maier,* Helv. *60*, 2213 (1977); *F. Brogli, E. Heilbronner, V. Hornung & E. Kloster-Jensen,* Helv. *56*, 2171 (1973).
[15] *R.G. Cooks, J.H. Beynon, R.M. Caprioli & G.R. Lester,* 'Metastable Ions', Elsevier, Amsterdam 1973.
[16] *F.P. Lossing,* Canad. J. Chemistry *50*, 3973 (1972).
[17] *P. Carlier, J.E. Dubois, P. Masclet & G. Mouvier,* J. Electron Spectrosc. *7*, 55 (1975).
[18] *A.S. Werner & T. Baer,* J. chem. Physics *62*, 2900 (1975).
[19] *S.W. Benson, F.R. Cruigkshank, D.M. Golden, G.R. Haugen, H.E. O'Neal, A.S. Rodgers, R. Shaw & R. Walsh,* Chem. Rev. *69*, 279 (1969); *S.W. Benson,* 'Thermochemical Kinetics', J. Wiley and Sons, New York 1968.
[20] *T. Baer, G.D. Willett, D. Smith & J.S. Phillips,* J. chem. Physics *70*, 4076 (1979).
[21] *I. Howe & F.W. McLafferty,* J. Amer. chem. Soc. *93*, 99 (1971).
[22] *A.C. Parr, A.J. Jason & R. Stockbauer,* Int. J. Mass Spectrom. Ion Physics *26*, 23 (1978).
[23] *A.C. Parr, A.J. Jason, R. Stockbauer & K.E. McCulloh,* Int. J. Mass Spectrom. Ion Physics, *30*, 319 (1979).
[24] *J. Dannacher & J. Vogt,* Helv. *61*, 361 (1978).
[25] *L. Brandsma,* 'Preparative Acetylenic Chemistry', Elsevier Publishing Company, Amsterdam, London, New York 1971.
[26] *J.C. Lavalley & J. Saussey,* in 'Chemistry of the Functional Groups, The Chemistry of the Carbon-Carbon-Triple-Bond', Chapter 20 (S. Patai, Edit.), J. Wiley and Sons, New York 1978.
[27] *T. Bally, H. Baumgärtel, U. Büchler, E. Haselbach, W. Lohr, J.P. Maier & J. Vogt,* Helv. *61*, 741 (1978); *U. Büchler & J. Vogt,* Org. Mass Spectr. *14*, 503 (1979).
[28] *J. Dannacher, A. Schmelzer, J.P. Stadelmann & J. Vogt,* Int. J. Mass Spectrom. Ion Physics *31*, 175 (1979).